Correlation Between Morphology and Field-Effect-Transistor Mobility in Tetracene Thin Films

Cicoira, Fabio; Santato, Clara; Dinelli, Franco; Murgia, Mauro; Loi, Maria Antonietta; Biscarini, Fabio; Zamboni, Roberto; Heremans, Paul; Muccini, Michele

Published in:
Advanced Functional Materials

DOI:
10.1002/adfm.200400278

ADVANCED FUNCTIONAL MATERIALS

Correlation Between Morphology and Field-Effect-Transistor Mobility in Tetracene Thin Films**

By *Fabio Cicoira*,* *Clara Santato*, *Franco Dinelli*, *Mauro Murgia*, *Maria Antonietta Loi*, *Fabio Biscarini*, *Roberto Zamboni*, *Paul Heremans*, and *Michele Muccini**

The growth of vacuum-sublimed tetracene thin films on silicon dioxide has been investigated from the early stages of the process. The effects of deposition flux and substrate silanization on film morphology and electrical properties have been explored. Tetracene shows an island growth, resulting in films with a granular structure. Both an increase in the deposition flux and the substrate silanization determine a decrease of the grain size and an improvement of the connectivity of the film in direct contact with the substrate. The hole mobility in field-effect transistors based on tetracene thin films, which also generate electroluminescence, increases with the deposition flux and values as high as 0.15 $cm^2 V^{-1} s^{-1}$ are obtained.

1. Introduction

Organic thin films are of great interest for use as active layers in electronic devices such as field-effect transistors (FETs), light-emitting diodes (LEDs), and photovoltaic cells.[1] One of the features making them attractive is multifunctionality, i.e., the possibility of combining electronic and optoelectronic properties in a single device. Therefore the search for organic materials having both good charge-transport and luminescence properties in thin films is an important topic. Tetracene is a good candidate for the purpose. Both single-crystal and thin-film tetracene-based FETs have been recently reported. A hole mobility of up to 0.4 $cm^2 V^{-1} s^{-1}$ has been measured in a tetracene single crystal,[2] whereas a hole mobility of up to 0.1 $cm^2 V^{-1} s^{-1}$ has been obtained on silicon dioxide (SiO_2) treated with octadecyltrichlorosilane (OTS) maintained at 15 °C during deposition.[3] In addition, tetracene exhibits a reasonably high fluorescence quantum yield both in single crystals[4] and in thin films.[5] Recently, light-emitting (field-effect) transistors (LETs) based on tetracene thin films have been produced.[6]

The effects of film morphology on the electrical properties of tetracene-based field-effect devices have yet to be deeply investigated. With this work, we intend to address this important topic. The morphology of organic thin films is related to several parameters such as deposition flux and substrate temperature during deposition,[7] and also to substrate surface treatment, e.g., the surface self-assembly of organic monolayers (SAMs) with different terminations.[8] Here, we report on tetracene films grown at various deposition fluxes on SiO_2 and OTS-silanized SiO_2 (OTS/SiO_2) dielectric surfaces. The morphology of the films was studied as a function of the deposition flux and the substrate treatment. The FET hole mobility and LET external quantum efficiency were measured as a function of the deposition flux.

2. Results

2.1. Morphology

Figure 1 shows atomic force microscopy (AFM) images of films deposited on SiO_2 (left column) and OTS/SiO_2 (right column) varying the deposition flux (F) from 0.02 to 10 Å s^{-1}. The nominal thickness of the films is 50 nm, a typical value for active layers in organic thin-film-based devices. The images show the effects of the deposition flux and substrate treatment: i) on a given substrate, the grain size decreases with increasing deposition flux; ii) at a given deposition flux, the grain size is smaller on OTS/SiO_2; and iii) OTS favors the formation of grains with a more regular shape and size distribution. Complete substrate coverage is achieved at all deposition fluxes, with the exception of 0.02 Å s^{-1} on SiO_2. In this case, large islands randomly distributed, as shown in Figure 1a, are typically observed. Such islands exhibit a faceted shape, lateral dimensions of a few micrometers, and a thickness of a few hundreds of nanometers, clear indications of a three-dimensional growth.

An estimation of the average grain size can be achieved by the evaluation of the correlation length (ξ) through power-spectrum density analysis.[9] ξ is the characteristic distance

[*] Dr. F. Cicoira, Dr. M. Muccini, Dr. C. Santato, Dr. F. Dinelli, Dr. M. Murgia, Dr. M. A. Loi, Dr. F. Biscarini, Dr. R. Zamboni, Consiglio Nazionale delle Ricerche (CNR)
Istituto per lo Studio dei Materiali Nanostrutturati (ISMN)
Sezione di Bologna, Via Gobetti 101, I-40129 Bologna (Italy)
E-mail: f.cicoira@ism.bo.cnr.it, M.Muccini@ism.bo.cnr.it
Dr. P. Heremans
IMEC
Kapeldreef 75, B-3001 Leuven (Belgium)
Dr. P. Heremans
Katholieke Universiteit Leuven, Electrical Engineering Department, Kasteelpark Arenberg 10, B- 3001 Leuven (Belgium)

[**] The authors acknowledge the EU-IST-FET program under project IST-33057 (ILO) for financial support, and Prof. Peter Stallinga (Universidade do Algarve, Faro, Portugal), Dr. Patrik Hoffmann and Laura Barbieri (Swiss Federal Institute of Technology Lausanne, EPFL), and Dr. Siegfried Karg and Constance Rost (IBM Zürich Research Laboratory) for fruitful discussions.

 DOI: 10.1002/adfm.200400278

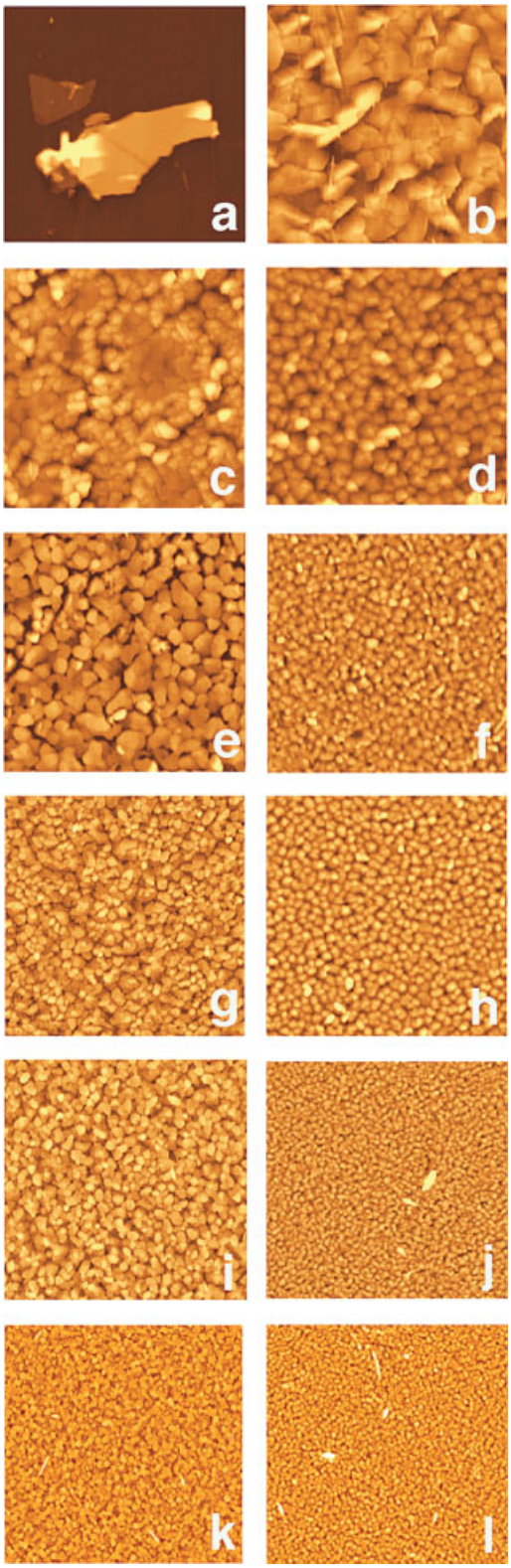

Figure 1. 10 μm × 10 μm AFM images of 50 nm thick (nominal thickness) tetracene films deposited on SiO_2 (left column) and OTS/SiO_2 (right column) at a nominal deposition flux of 0.02 Å s^{-1} (a,b), 0.1 Å s^{-1} (c,d), 0.5 Å s^{-1} (e,f), 2 Å s^{-1} (g,h) 5 Å s^{-1} (i,j), and 10 Å s^{-1} (k,l). Height ranges: 0-250 nm (a), 0-600 nm (b), 0-250 nm (c), 0-300 nm (d), 0-150 nm (e), 0-200 nm (f), 0-60 nm (g), 0-100 nm (h), 0-70 nm (i), 0-70 nm (j), 0-55 nm (k), and 0-60 nm (l).

between grains and, therefore, in completely connected films, corresponds, to a good approximation, to the grain size. Moreover, ξ scales to the inverse square root of the surface density of the islands. Figure 2 reports ξ (on the left y-axis) and the root-mean-square (rms) roughness (on the right y-axis) versus the nominal deposition flux (F) for films grown on SiO_2 and OTS/SiO_2. The plot shows that ξ decreases with increasing deposition flux following a power law. At any given deposition flux, ξ is smaller for OTS/SiO_2. The rms roughness follows a similar trend.

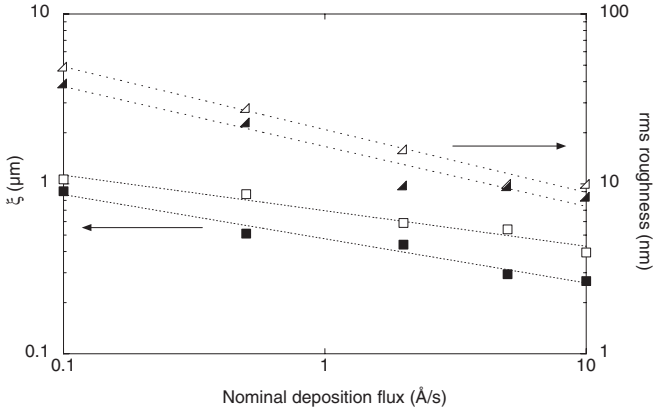

Figure 2. Correlation length (ξ) versus nominal deposition flux (left y-axis) and rms roughness (right y-axis) for 50 nm thick (nominal thickness) tetracene films deposited on SiO_2 (open symbols) and OTS/SiO_2 (filled symbols). The dotted lines correspond to the fit of the experimental data with a power law.

To investigate the effect of the deposition flux and the substrate treatment on the early stages of growth, the morphology at low nominal thicknesses (d) was also studied. Figure 3 shows images of films grown at 0.5 Å s^{-1} with increasing nominal thickness from 1 to 20 nm. Films deposited on SiO_2 and OTS/SiO_2 are reported in the left and right column, respectively. On both substrates, tetracene shows a three-dimensional island growth.[10] Complete substrate coverage is achieved at a nominal thickness between 10 and 20 nm. The OTS treatment does not change the growth mode but strongly influences the island density and size. This effect is already clear for a nominal film thickness of 1 nm, and becomes more evident for higher thicknesses. In 3, 5, and 10 nm thick films on OTS/SiO_2, the islands exhibit a higher density and a more regular size distribution. At very low coverage ($d < 10$ nm), the islands are higher than 70 nm on both substrates, indicating a three-dimensional growth. On SiO_2, a morphological transition from islands to grains with a more regular shape and size distribution occurs at a nominal thickness between 10 and 20 nm. This transition is not observed for the corresponding films grown on OTS/SiO_2.

The variation of the nucleation density with nominal thickness can be estimated from a plot of ξ versus the nominal thickness. The plot reported in Figure 4 shows that the island density of films grown at 0.5 Å s^{-1} increases with increasing nominal thickness, with a sharper increase between 1 and

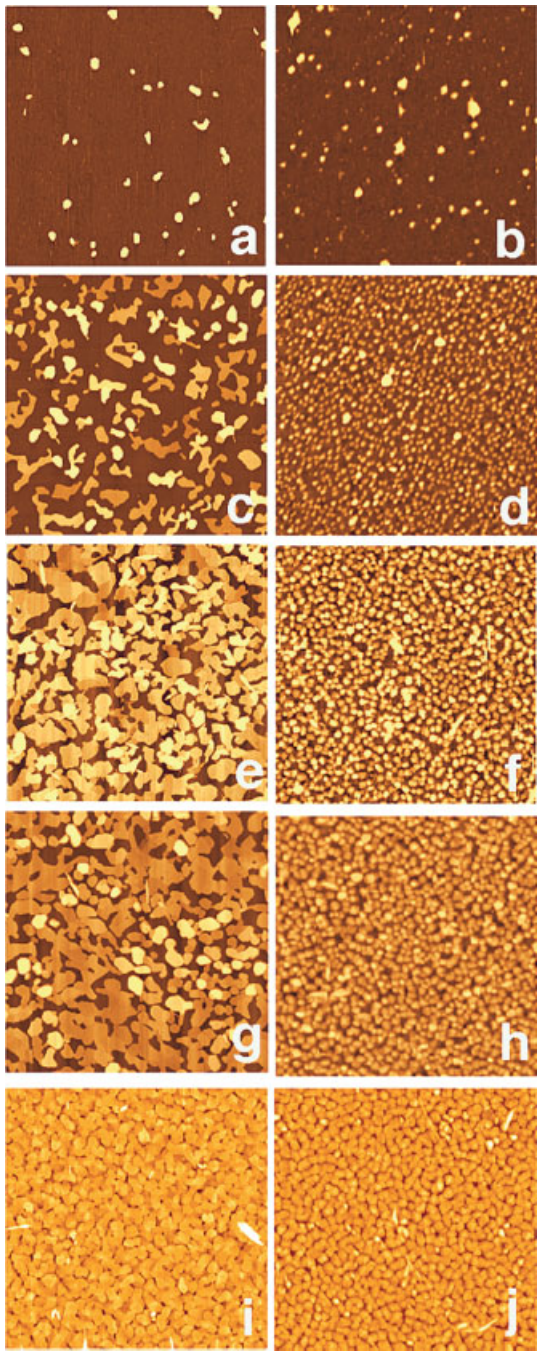

Figure 3. 10 μm × 10 μm AFM images of films grown at a nominal deposition flux of 0.5 Å s^{-1}, on SiO_2 (left column) and OTS/SiO_2 (right column) having nominal thicknesses of 1 nm (a,b), 3 nm (c,d), 5 nm (e, f), 10 nm (g,h), and 20 nm (i,j). Height ranges: 0-70 nm (a), 0-80 nm (b), 0-100 nm (c), 0-130 nm (d), 0-70 nm (e), 0-100 nm (f), 0-100 nm (g), 0-140 nm (h), 0-70 nm (i), and 0-100 nm (j).

3 nm. On OTS/SiO_2 the island density show higher values and reaches a stable value already at a thickness of 3 nm.

The effect of the deposition flux on the early stages of growth is shown in Figure 5. Here we compare films deposited on SiO_2 at 0.1 (a), 0.5 (b), and 5 Å s^{-1} (c), each with a nominal thickness of 10 nm. A higher deposition flux strongly improves

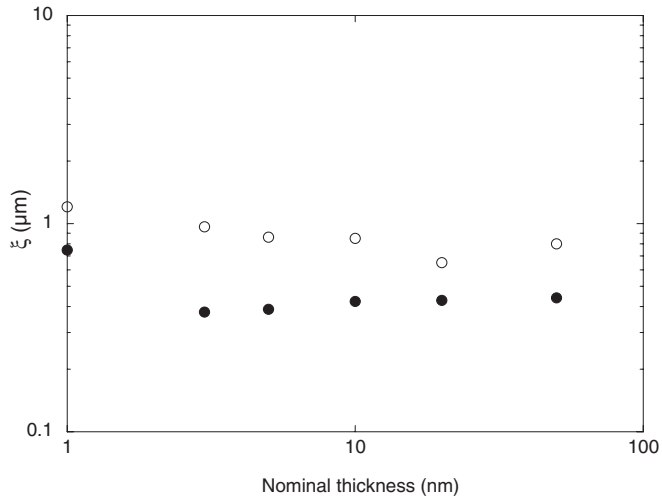

Figure 4. Correlation length (ξ) versus nominal film thickness for tetracene films grown at a nominal deposition flux of 0.5 Å s^{-1}, on SiO_2 (open symbols) and OTS/SiO_2 (filled symbols).

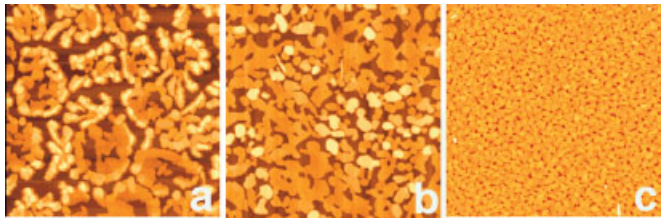

Figure 5. 5 μm × 5 μm AFM images of tetracene films grown on SiO_2 at nominal deposition fluxes of 0.1 Å s^{-1} (a), 0.5 Å s^{-1} (b), and 5 Å s^{-1} (c), each having a nominal thickness of 10 nm.

film connectivity and substrate coverage during the early stages of growth.

Information on the crystalline-domain orientation in the films is provided by laser scanning confocal microscopy (LSCM). Tetracene crystals are triclinic with two molecules in the unit cell.[11] X-ray diffraction of thin films on SiO_2 showed a similar unit cell with the molecules oriented almost perpendicular to the substrate.[3] Bearing this in mind, if the fluorescence of a sample of uniform thickness is excited with a laser having controlled in-plane polarization, changes in the fluorescence intensity can give an indication on the orientation of the crystalline domains. Figure 6 reports LSCM images of 50 nm thick films grown at 0.1 Å s^{-1} (b) and 10 Å s^{-1} (d), and, for comparison, AFM images of the same samples (Figs. 6a,c). The LSCM micrograph of the film deposited at lower flux highlights the coexistence of domains with different fluorescence intensities. The corresponding AFM image shows that all the domains have a similar thickness. Therefore, the different fluorescence intensity is attributed to different crystalline orientations of the domains, with brighter regions corresponding to crystalline orientation more favorable for laser excitation. Figure 6d shows that in the film deposited at higher flux, such large domains tend to disappear.

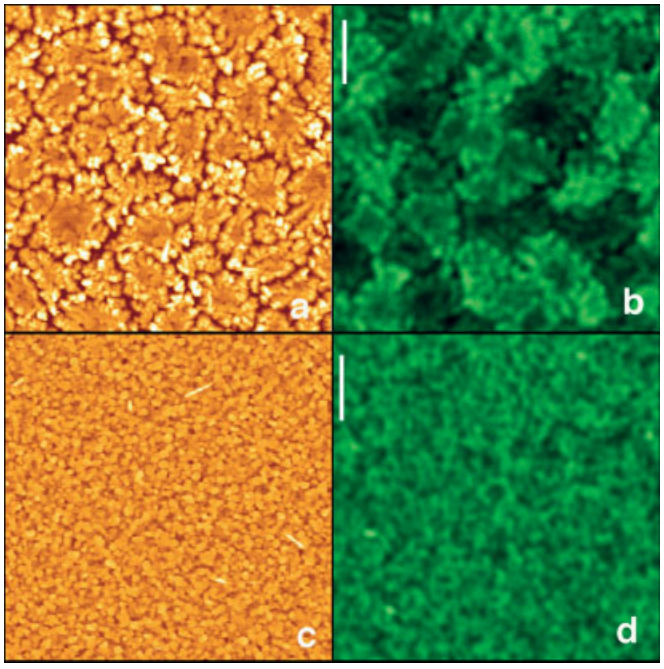

Figure 6. 20 μm × 20 μm AFM (a,c) and LSCM images (b,d) of tetracene films grown on SiO_2 at nominal deposition fluxes of 0.1 Å s^{-1} (a,b) and 10 Å s^{-1} (c,d), having a nominal thickness of 50 nm. The polarization direction of the laser light is indicated by the line in the LSCM images.

2.2. Field-Effect Mobility and Electroluminescence

The drain–source current (I_{ds}) and electroluminescence (EL) of tetracene-based LETs were measured as a function of the deposition flux of the active layer.

Figure 7 reports the I_{ds} and EL of a tetracene LET, simultaneously collected, as a function of the drain–source voltage (V_{ds}) at different gate–source voltages (V_{gs}) for a 50 nm-thick film grown at 5 Å s^{-1}. The device structure and bias conditions are shown in Scheme 1. The I_{ds}–V_{ds} plots show the typical behavior of a p-type FET working in accumulation mode. At a fixed V_{gs}, for low $|V_{ds}|$, $|I_{ds}|$ increases with $|V_{ds}|$ and then attains saturation ($I_{ds,sat}$) at larger $|V_{ds}|$. $|I_{ds,sat}|$ increases with an increase of $|V_{gs}|$.

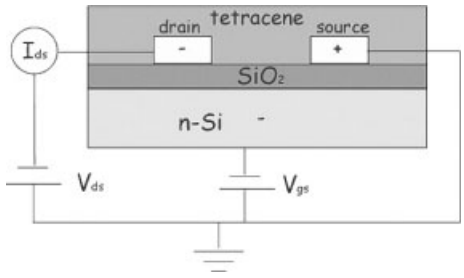

Scheme 1. The structure of an LET indicating drain–source current (I_{ds}), drain–source voltage (V_{ds}), and gate–source voltage (V_{gs}).

The onset of EL, for a fixed V_{gs}, is at more negative voltages than the onset of I_{ds}. The EL continuously increases with $|V_{ds}|$, being modulated by V_{gs}.

The FET mobility (μ) is calculated at saturation by using the equation:

$$\left|I_{ds,sat}\right| = \frac{W}{2L}\mu C_i (V_{gs} - V_T)^2 \quad (1)$$

where W and L are the channel width and length, respectively, C_i is the SiO_2 capacitance per unit area (3.45×10^{-8} F cm^{-2} for 100 nm-thick SiO_2), and V_T is the threshold voltage[12] deduced from the intercept at $y = 0$ of the $(|I_{ds,sat}|)^{1/2}$ versus V_{gs} plot.

The OTS treatment does not significantly improve the LET electrical performance, therefore only measurements on LETs deposited on SiO_2 are reported below.

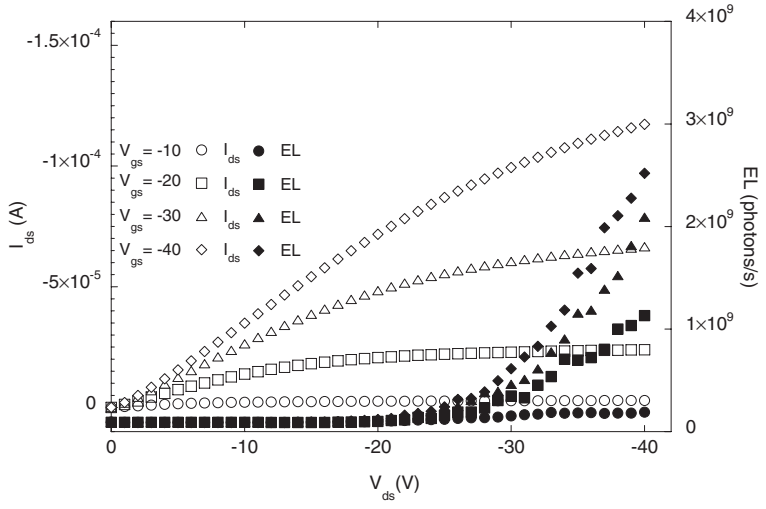

Figure 7. Drain–source current (I_{ds}), on the left y-axis, and electroluminescence (EL), on the right y-axis, versus drain–source voltage (V_{ds}), recorded at various gate–source voltages (V_{gs}). Tetracene LET with $W/L = 1029/3$, nominal thickness 50 nm, and nominal deposition flux 5 Å s^{-1}.

The dependence of the mobility on the deposition flux is shown in Figure 8. Each reported value is the average for 10–15 devices available on the substrate. The average mobility clearly increases with increasing deposition flux between 0.1 and 3 Å s^{-1}. A further increase of the deposition flux does not significantly affect the mobility. Values higher than 0.1 $cm^2 V^{-1} s^{-1}$ were obtained for films deposited at 5 and 10 Å s^{-1}. The best mobility values on OTS/SiO_2 can also be as high as 0.1 $cm^2 V^{-1} s^{-1}$, suggesting that the improvement in surface coverage and film connectivity induced by OTS could be compensated by surface contamination occurred during hydration and/or liquid-phase silanization. These values are comparable with those obtained by Gundlach et al.[3] on OTS/SiO_2 held at 15 °C during deposition. The external quantum efficiency of electroluminescence is found to be independent of the deposition flux. This finding is not surprising in view of the mechanism of light generation in LETs.[13] A higher hole current leads to higher

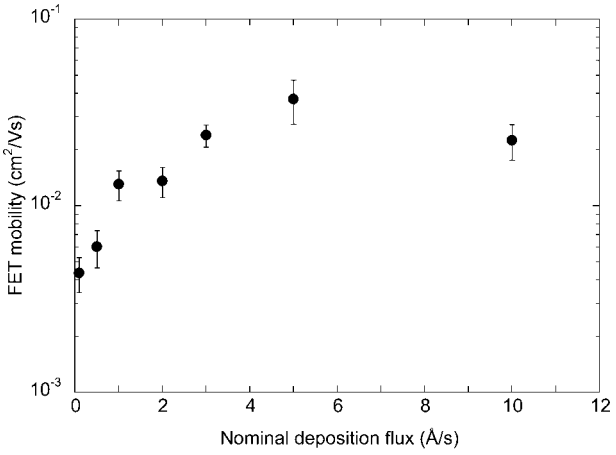

Figure 8. FET mobility of tetracene-based LETs versus nominal deposition flux. On each substrate the mobility was averaged over 10–15 devices with channel lengths (L) of 2, 3, 5, and 20 μm and widths (W) of 100, 300, 1019, 1029, and 1048 μm. The nominal thickness of the active layer is 50 nm. The error bars are two times the standard error.

electroluminescence intensity but does not affect the device efficiency (photon/charge), which depends on the electron injection from the drain electrode via tunneling.

3. Discussion

Film formation from the vapor phase can be described as follows. Molecules from the gas phase reach the substrate with a flux $F = P(2\pi MkT)^{-1/2}$ where P is the gas pressure, M the molecular weight, k the Boltzmann constant, and T the source temperature. The molecules then diffuse on the surface where they may undergo several processes, namely (assuming an ideally flat substrate) nucleation, capture by existing nuclei (growth), or re-evaporation. The growth mode of the film is determined by the balance between surface, interfacial, and strain energies in the film–substrate system.[10] Tetracene films on SiO_2 and OTS/SiO_2 at room temperature show an island growth, in agreement with recently published theoretical calculations.[14] This type of growth is tentatively explained by a weak film–substrate interaction and a strong strain in the film.[15] In island-growth systems, no or little deposition occurs at low deposition flux (low supersaturation). Increasing the deposition flux (high supersaturation) allows the growth of continuous films. The growth process is then governed by kinetic processes, such as deposition flux, surface diffusion, nucleation and binding to existing clusters.

The island density and size are related, by a power law, to the ratio (F/D_s), where D_s is the surface diffusion coefficient of the molecules on the substrate.[16] As shown in Figure 2, by increasing the deposition flux the island size decreases whereas the island density increases, leading to an improvement in substrate coverage. The OTS treatment, at any given deposition flux, induces an increase of the island density and a decrease of the island size. This effect can be attributed to thermodynamic effects, as reduced strain in the film, or kinetic effects, as a decrease of the surface diffusion coefficient for tetracene. The morphological transition observed in Figure 3 after complete substrate coverage could originate from a change of the surface energy and/or surface diffusion coefficient occurring when tetracene grows on a pre-deposited tetracene layer. This transition is not observed on OTS/SiO_2, probably because the above-mentioned changes are less pronounced. In Figure 4, the fact that the correlation length on OTS/SiO_2 remains constant, except at low coverage, could indicate that nucleation occurs at defects, rather than being diffusion-limited.

The electrical measurements indicate that high hole FET mobility (> 0.1 cm^2 V^{-1} s^{-1}) in tetracene LETs on SiO_2 can be achieved at a high deposition flux of the active layer (> 3 Å s^{-1}). On the one hand, as charge transport occurs within a thin layer next to the organic–dielectric interface,[1b,17] the uniform substrate coverage obtained at high fluxes facilitates charge transport. On the other hand, the decrease in grain size increases the density of grain boundaries, expected to be detrimental for charge transport. Indeed, grain boundaries are known to act as traps for charge carriers.[12a] The correlation between FET mobility and deposition flux suggests that, for tetracene films on SiO_2, a more uniform substrate coverage dominates over the density of grain boundaries in determining FET mobility.

Our data show that high FET mobilities in tetracene films, similar to the highest values reported for films grown at low temperature on OTS/SiO_2,[3] can be achieved by depositing the films at high deposition flux onto SiO_2 substrates (UV/O_3 cleaned) kept at room temperature. The OTS treatment, which has a clear effect on film morphology, has no significant effect on the mobility, unlike previously published works on tetracene[3] and pentacene[8a] FETs.

4. Conclusions

Vacuum-sublimed tetracene films grown on SiO_2 and OTS/SiO_2 show an island growth. An increase of deposition flux and the OTS treatment both lead to an increase of the island density, a more uniform substrate coverage, and an improvement in film connectivity. After complete substrate coverage, tetracene films exhibit a polycrystalline structure with randomly oriented grains. The hole FET mobility in tetracene LETs increases with an increasing deposition flux of the active layer and then reaches a plateau at higher fluxes. Values as high as 0.15 cm^2 V^{-1} s^{-1} were measured in films deposited at 5 Å s^{-1}. The OTS treatment does not improve the mobility. The increase of the hole FET mobility with increasing deposition flux can be explained with a more uniform substrate coverage during the early stages of film growth. Despite the increase of the density of the grain boundaries, small well-interconnected grains lead to a more efficient charge transport.

5. Experimental

Tetracene (TCI, 98%) was used as received. The films were grown by vacuum-sublimation in a system with a base pressure of about 5×10^{-7} mbar. Nominal thickness and deposition flux were monitored using a quartz crystal microbalance placed nearby the substrate. Two different types of substrates were used. For morphological analysis, films were deposited onto 100 nm thick SiO_2 thermally grown on heavily n-doped (As) Si. For electrical and optoelectronic characterizations, films were deposited onto 100 nm thick SiO_2, thermally grown on heavily n-doped (As) Si, pre-patterned with Au source/drain bottom contacts, formed by sputtering a 30 nm Au layer. Patterning was achieved by a lift-off process. Ultrathin Au electrodes with no adhesion layer ensured charge injection to occur from gold, and prevented shadow effects when subliming the organic ultrathin film. Gold-electrode profiles were checked using AFM to have smooth slopes and to be highly regular along the entire channel width. Heavily doped n-Si was used as gate electrode. The nominal thickness of the active layer was fixed at 50 nm. On each substrate the FET mobility was averaged over 10–15 devices with channel lengths (L) of 2, 3, 5, and 20 μm and widths (W) of 100, 300, 1019, 1029, and 1048 μm. The substrates were cleaned by sonication in acetone followed by UV/O_3 exposure. Silanization was performed by dipping the substrates, after hydration, into an OTS solution in dry toluene, under a N_2 atmosphere. The substrates were kept at room temperature during film deposition.

The film morphology was studied with an atomic force microscope (AFM, Park, CP model) in contact mode with Si_3N_4 cantilevers (Nanoprobes) that had a spring constant of 0.1 N m^{-1}. Fluorescence imaging of the samples was performed with a laser scanning confocal microscope (LSCM, Nikon TE 2000) [79], where fluorescence was excited at 488 nm with an Ar^+ laser beam with controlled in-plane polarization. Sample imaging was achieved by scanning the laser spot on the sample while keeping a constant polarization direction of the fluorescence exciting laser beam. The fluorescence intensity of the images was therefore sensitive to the crystallographic orientation of domains.

FET measurements were carried out at room temperature, in an N_2-purged glove-box. The devices were operated as p-type FETs, working in accumulation mode. All of them were able to generate electroluminescence. A DC power supply (Agilent 6634B) was used to bias the gate (V_{gs}), whilst a source-measure unit (Keithley 236) controlled the drain–source voltage (V_{ds}) and measured the drain–source current (I_{ds}). Optoelectronic measurements were carried out under high vacuum (10^{-5} mbar) inside a calibrated integrating sphere where high-sensitivity light detection was achieved through a pre-amplified photomultiplier [18]. In order to avoid ageing effects, all the measurements were performed on freshly prepared samples.

Received: June 25, 2004
Final version: September 25, 2004

[1] a) F. Garnier, G. Horowitz, X. Peng, D. Fichou, *Adv. Mater*. **1990**, *2*, 592. b) A. Dodabalapur, L. Torsi, H. E. Katz, *Science* **1995**, *268*, 270. c) C. W. Tang, S. A. Van Slyke, *Appl. Phys. Lett.* **1987**, *51*, 913. d) N. S. Sariciftci, L. Smilowitz, A. J. Heeger, F. Wudl, *Science* **1992**, *258*, 1474.

[2] R. W. I. de Boer, A. F. Morpurgo, T. M. Klapwijk, *Appl. Phys. Lett.* **2003**, *83*, 4345.

[3] D. J. Gundlach, J. A. Nichols, L. Zhou, T. N. Jackson, *Appl. Phys. Lett.* **2002**, *80*, 2925.

[4] M. Pope, C. E. Swenberg, in *Electronic Processes in Organic Crystal and Polymers*, 2nd ed., Oxford University Press, Oxford, UK **1999**, Ch. 3.

[5] S. H. Lim, T. G. Bjorklund, F. C. Spano, C. J. Bardeen, *Phys. Rev. Lett.* **2004**, *92*, 107 402.

[6] A. Hepp, H. Heil, W. Weise, M. Ahles, R. Schmechel, H. von Seggern, *Phys. Rev. Lett.* **2003**, *91*, 157 406.

[7] a) G. Horowitz, M. E. Hajlaoui, *Adv. Mater*. **2000**, *12*, 1046. b) M. Muccini, M. Murgia, F. Biscarini, C. Taliani, *Adv. Mater.* **2001**, *13*, 355. c) F. Biscarini, R. Zamboni, P. Samorì, P. Ostoja, C. Taliani, *Phys. Rev. B* **1995**, *52*, 14 868. d) C. D. Dimitrakopoulos, A. R. Brown, A. Pomp, *J. App. Phys.* **1996**, *4*, 2501. e) M. H. Choo, J. H. Kim, S. Im, *Appl. Phys. Lett.* **2002**, *81*, 4640. f) B. J. Chen, W. Y. Lai, Z. Q. Gao, C. S. Lee, S. T. Lee, W. A. Gambling, *Appl. Phys. Lett.* **1999**, *75*, 4010. g) M. A. Loi, E. Da Como, F. Dinelli, M. Murgia, R. Zamboni, F. Biscarini, M. Muccini, *Nat. Mater*. **2005**, 4, 81

[8] a) M. Shtein, J. Mapel, J. B. Benzinger, S. R. Forrest, *Appl. Phys. Lett.* **2002**, *81*, 268. b) A. Salleo, M. L. Chabinyc, M. S. Yang, R. A. Street, *Appl. Phys. Lett.* **2002**, *81*, 4383. c) X. Liu, S. H. Mohamed, J. M. Ngaruiya, M. Wuttig, T. Michely, *J. Appl. Phys.* **2003**, *93*, 4852.

[9] F. Biscarini, P. Samorì, O. Greco, R. Zamboni, *Phys. Rev. Lett.* **1997**, *12*, 2389.

[10] J. A. Venables, G. T. D. Spiller, *Rep. Prog. Phys.* **1984**, *47*, 400.

[11] R. B. Campbell, J. M. Robertson, *Acta Cryst.* **1962**, *15*, 289.

[12] a) G. Horowitz, R. Hajlaoui, H. Bouchriha, R. Bourguiga, M. Hajlaoui, *Adv. Mater.* **1998**, *10*, 923. b) N. Karl, in *Organic Electronic Materials* (Eds.: R. Farchioni, G. Grosso), Springer-Verlag, Berlin, Germany **2001**, Ch. 6.

[13] C. Santato, R. Capelli, M. A. Loi, V. A. L. Roy, P. Stallinga, F. Cicoira, M. Murgia, R. Zamboni, C. Rost, S. F. Karg, M. Muccini, *Synth. Met*. **2004**, *146*, 329.

[14] S. Verlaak, S. Steudel, P. Heremans, D. Janssen, M. S. Deleuze; *Phys. Rev. B* **2003,** *68*, 195 409.

[15] a) Q. Chen, T. Rada, T. Bitzer, N. V. Richardson, *Surf. Sci.* **2003** *547*, 385. b) F. Schreiber, *Phys. Stat. Sol. A* **2004**, *201*, 1037.

[16] B. Krause, A. C. Duerr, K. Ritley, F. Schreiber, H. Dosch, D. Smilgies, *Phys. Rev. B* **2002,** *66*, 235 404.

[17] a) G. Horowitz *Adv. Funct. Mater.* **2003**, *13*, 53. b) F. Dinelli, M. Murgia, P. Levy, M. Cavallini, F. Biscarini, D. M. De Leeuw, *Phys. Rev. Lett.* **2004**, *92*, 116 802.

[18] P. Mei, M. Murgia, C. Taliani, E. Lunedei, M. Muccini, *J. Appl. Phys.* **2000**, *88*, 5158.

